AJNR Am J Neuroradiol 21:503–508, March 2000

Intraventricular CSF Pulsation Artifact on Fast Fluid-Attenuated Inversion-Recovery MR Images: Analysis of 100 Consecutive Normal Studies

Rohit Bakshi, Shelton D. Caruthers, Vallabh Janardhan, and Mohammad Wasay

BACKGROUND AND PURPOSE: **CSF pulsation artifact is a pitfall of fast fluid-attenuated inversion-recovery (FLAIR) brain MR imaging. We studied ventricular CSF pulsation artifact (VCSFA) on axial FLAIR images and its relationship to age and ventricular size.**

METHODS: **Fast FLAIR axial images were obtained on a 1.5-T unit (8000/150/2 [TR/TE/excitations], inversion time = 2200, field of view = 24 cm, matrix = 189 × 256, and 5-mm interleaved sections). Two observers rated VCSFA (hyperintensity on FLAIR images) in the lateral, third, and fourth ventricles by using a three-point ordinal scale in 100 consecutive subjects (ages 20–86 years) with normal brain MR studies. Left-to-right third ventricular width was also measured.**

RESULTS: **Seventy-two subjects had VCSFA in at least one ventricular cavity. The fourth ventricle was the most common site of VCSFA (n = 58), followed by the third ventricle (n = 47) and the lateral ventricles (n = 13). VCSFA was usually severe in the third and fourth ventricles and less severe in the lateral ventricles. Fourth ventricular VCSFA was significantly associated with third ventricular VCSFA. Increasing third ventricular size and, to a lesser extent, increasing age was significantly associated with VCSFA. Ghost pulsation of VCSFA occurred across the brain parenchyma in the phase-encoding direction. VCSFA seen in the fourth ventricle on axial FLAIR images disappeared on sagittal FLAIR images in one subject.**

CONCLUSION: **VCSFA on axial FLAIR images represents inflow artifact caused by inversion delay and ghosting effects. VCSFA might obscure or mimic intraventricular lesions, especially in the third and fourth ventricles. Although common in adults of all ages, VCSFA is associated with advancing age and increasing ventricular size. Thus, altered CSF flow dynamics that occur with ventriculomegaly and aging contribute to VCSFA on axial FLAIR MR images.**

The development of fluid-attenuated inversion-recovery (FLAIR) MR imaging (1) and the ability to perform FLAIR imaging with fast spin-echo (FSE) sequences (2) has markedly improved the MR diagnosis of a variety of brain disorders as compared with conventional MR imaging (3). The utility of FLAIR imaging relates to its sensitivity in depicting lesions causing T2 prolongation against a suppressed CSF background. The superiority of FLAIR imaging as compared with T1- and T2-weighted imaging has been suggested in the evaluation of a variety of disorders, such as stroke (4), multiple sclerosis (5), infections (6), hypertensive encephalopathy (7), and cerebral hemorrhage (8). One of the major limitations of FLAIR imaging, however, is ventricular CSF pulsation artifact (VCSFA) (3). This artifact could compromise the sensitivity and specificity of FLAIR images by leading to false-negative or false-positive interpretations of ventricular abnormalities. Thus, it is necessary to know the spectrum of the normal appearance of VCSFA. Our purpose was to describe the location, frequency, and severity of VCSFA on axial fast FLAIR MR brain images in 100 consecutive healthy adult subjects and to determine the relationship of VCSFA to age and ventricular size.

Received June 14, 1999; accepted after revision October 8.

From the Dent Neurologic Institute, Lucy Dent Imaging Center, Kaleida Health-Millard Fillmore Hospital, Buffalo, NY (R.B., V.J., M.W.); and Philips Medical Systems, Magnetic Resonance Division, Boston, MA (S.D.C.).

Address reprint requests to Rohit Bakshi, MD, Neuroscience Center E-2, 100 High St, Buffalo, NY 14203.

Methods

Subjects

Our adult tertiary hospital MR computer database was reviewed to identify patients who underwent FLAIR brain imaging between April and October 1998 and whose results in the original reports were normal in all cases. All MR images were reviewed by two of us to ensure that findings were nor-

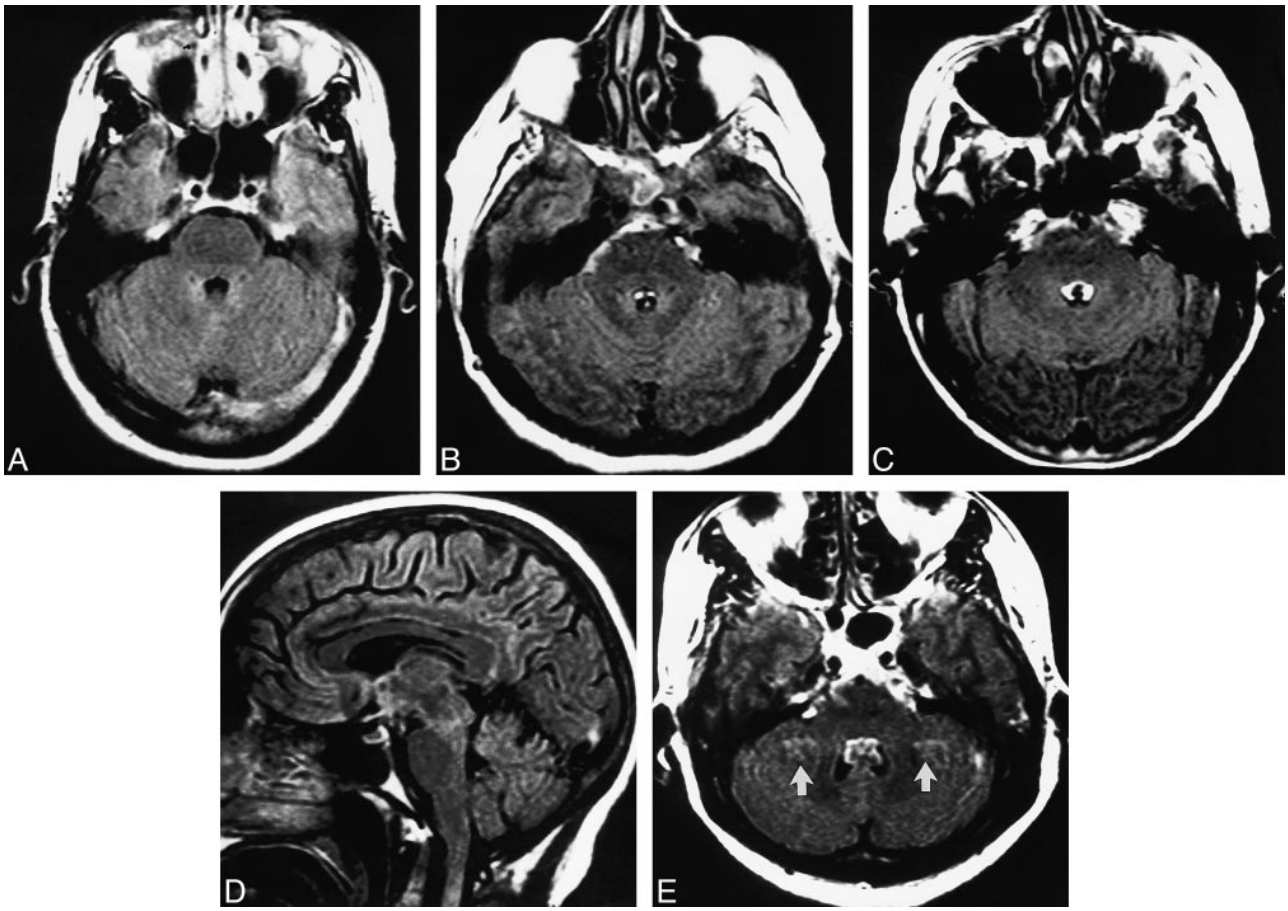

FIG 1. Fourth ventricular CSF pulsation artifact in four subjects.

A–C, FLAIR axial images of three patients show increasing severity of fourth ventricular CSF pulsation artifact with increasing age: grade 0 in a 32-year-old (*A*); grade 1 in a 43-year-old (*B*); and grade 2 in a 71-year-old (*C*). Subarachnoid CSF artifact is also present in the basal cisterns in *B* and *C.*

D, The fourth ventricular CSF pulsation artifact that was present on the axial FLAIR image (*C*) is not visible on this sagittal FLAIR image.

E, FLAIR axial image of a subject with fourth ventricular CSF pulsation artifact also shows ghost pulsation artifacts (*arrows*) in the phase-encoding axis (left to right), causing superimposition of hyperintensities on the bilateral cerebellar parenchyma.

mal on all pulse sequences. The study group included 100 consecutive subjects (70 women, 30 men) 20 to 86 years old (mean age ± SD, 48.0 ± 17.4). These patients underwent MR imaging for evaluation of headache, seizure disorder, tinnitus, or dizziness. The Human Research Committee at our institution approved this study.

Imaging

Fast FLAIR MR imaging was performed at 1.5 T as follows: 8000/150/2 (TR/TE/excitations), inversion time = 2200, turbo spin-echo factor (number of echoes) = 20, echo spacing = 12 milliseconds, field of view = 24 cm, matrix = 189 × 256, bandwidth = 217.3 Hz per pixel, 5-mm-thick axial sections, 20 slices, and a scan time of approximately 2 minutes. A multisection imaging technique was used with a section-selective inversion pulse. Multisection is an interleaved acquisition. The inversion pulse slice profile was as wide as the imaging slice profile (ie, 5 mm). A presaturation band was placed caudal to the image volume. At our institution, we have access to six MR scanners produced by four different vendors. We have seen similar-appearing VCSFA on axial FLAIR images from all of these scanners. For the current study, a single protocol using a single scanner was chosen. The protocol was developed the previous year to optimize lesion contrast with the fastest scanning time. The consequential trade-off was that we did not use gradient moment nulling (flow compensation), more robust inversion pulses, or other protocols that might have limited VCSFA (see Discussion).

To reduce variations in head position, we imaged all patients in the canthomeatal plane on the basis of the scout image. Subjects whose images were poor or contained motion artifact or head rotation were excluded. Two observers independently analyzed the 100 FLAIR MR images of the patients for the presence of VCSFA. We defined VCSFA as hyperintense signal in the ventricles that did not correspond to any normal anatomic structure. VCSFA for each patient was rated in three regions: the lateral ventricles, the third ventricle, and the fourth ventricle. Thus, 300 ratings were recorded for the 100 patients. A three-point ordinal rating scale was used for VCSFA in each region based on severity (Fig 1): grade 0 = normal hypointense signal; grade 1 = mild hyperintense signal; grade 2 = prominent/severe hyperintense signal. The severity of VCSFA was defined as the intensity (strength) of the abnormal signal. Interobserver agreement between the two raters was high, with only five differences among the 300 ratings (each within one point). These differences were resolved by consensus. To explore whether VCSFA was related to ventricular enlargement, third ventricular width was measured from left to right on the axial images. This width was determined along a plane corresponding to the (anteroposterior) midpoint of the ventricle

Ventricular CSF pulsation artifact on fast FLAIR MR images as related to sex, age, and size of third ventricle

Location and Severity of CSF Pulsation Artifact on Fast FLAIR MR Images	No. of Subjects			Mean Age (yrs)		Third Ventricular Diameter (mean mm ± SD)	
	Total (n = 100)	Male (n = 30)	Female (n = 70)	Male	Female	Male	Female
Lateral ventricles							
Grade 0	87	26	61	47	48	4.9 ± 2.7	3.7 ± 2.0
Grade 1	11	3	8	50	46	5.3 ± 2.3	4.0 ± 2.4
Grade 2	2	1	1	39	23	2.0 (n = 1)	3.0 (n = 1)
Third ventricle							
Grade 0	53	12	41	45	46	3.8 ± 1.5	3.2 ± 1.7
Grade 1	20	8	12	44	45	5.3 ± 2.1	3.2 ± 2.0
Grade 2	27	10	17	55	55	6.9 ± 3.4	5.5 ± 1.8
Fourth ventricle							
Grade 0	42	13	29	42	45	3.9 ± 1.6	3.3 ± 1.4
Grade 1	15	3	12	49	49	6.0 ± 2.0	4.2 ± 2.4
Grade 2	43	14	29	53	51	6.2 ± 3.3	4.1 ± 2.3

Note.—See Methods for descriptions of grades 0–2. FLAIR indicates fluid-attenuated inversion-recovery sequences.

by using a magnifying glass and electronic calipers. Intraobserver agreement regarding ventricular width measurements was determined by calculating the coefficient of variation as a percentage (SD/mean) for measurements made 1 month apart by one of us in 20 randomly selected cases. The mean coefficient of variation was 3% for the width of the third ventricle.

Statistical Analysis

The Spearman rank correlation test determined the relationship between VCSFA, age, and third ventricular size. The Fisher exact probability test was used to assess associations between the presence of VCSFA in a ventricular cavity (grade 1 or 2) and the presence of VCSFA in another ventricular cavity or sex. The Mann-Whitney *U* test or an analysis of variance assessed group differences (sex or the presence of VCSFA) in relation to severity of VCSFA, age, and third ventricular size. A *P* value less than .05 was considered statistically significant.

Results

Data showing the location, severity, and frequency of VCSFA in relation to ventricular size, age, and sex are presented in the Table and in Figures 1 through 4. Examples of VCSFA on FLAIR images are shown in Figures 1 through 3.

Frequency and Distribution of VCSFA

VCSFA was commonly found throughout the ventricular system at all ages (Table, Figs 1–3). Seventy-two percent (n = 72) of subjects had some degree of VCSFA in at least one ventricular cavity. Eight percent (n = 8) of subjects had VCSFA in all three ventricular cavities. The fourth ventricle

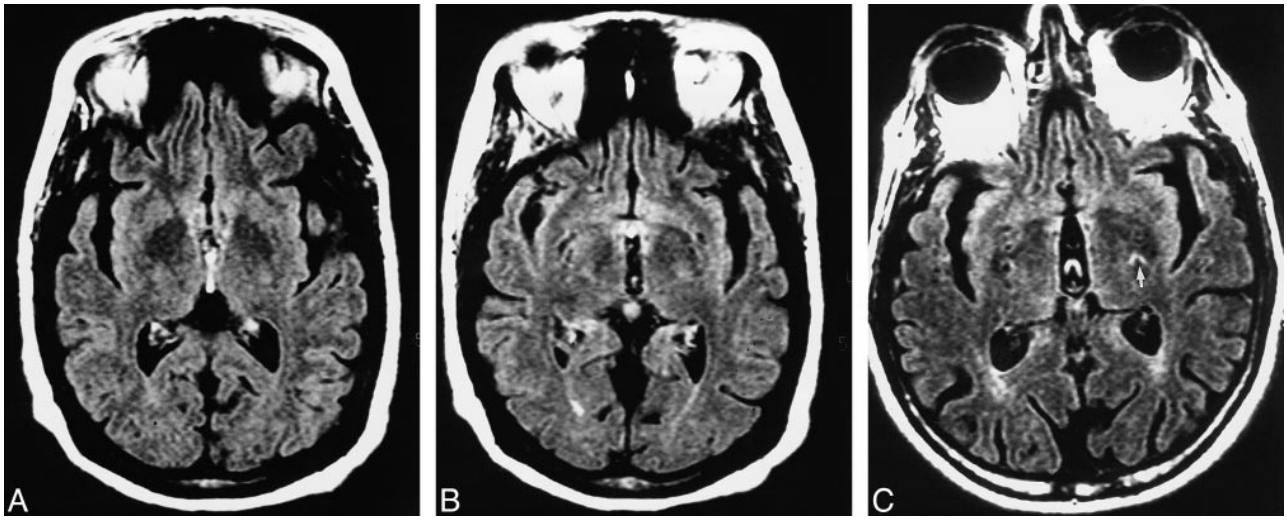

FIG 2. Third ventricular CSF pulsation artifact in two subjects.

A and *B,* Contiguous FLAIR axial images of a 67-year-old man referred for dizziness. The patient has a grade 2 third ventricular VCSFA in the inferior aspect of the third ventricle (*A*) and a large third ventricle.

C, FLAIR axial image of a subject with third ventricular CSF pulsation artifact also has bilateral ghost pulsation artifacts in the phase-encoding axis (left to right), causing superimposition of hyperintensities on the bilateral adjacent brain. The most prominent ghost artifact (*arrow*) is in the left basal ganglia.

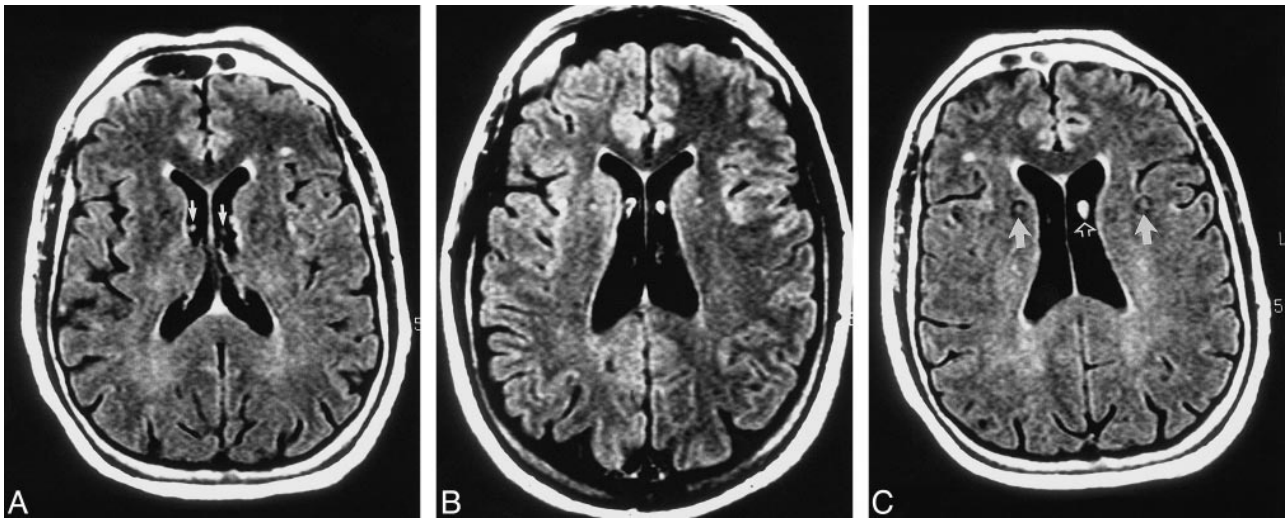

FIG 3. Lateral ventricular CSF pulsation artifact in two subjects.

A and *B*, Contiguous FLAIR axial images of a 70-year-old man show focal lateral ventricular CSF pulsation artifacts bilaterally, more prominent on the right, in the region of the foramen of Monro (*arrows*).

C, A subject with lateral ventricular CSF pulsation artifact (*open arrow*) also has ghost pulsation artifacts in the phase-encoding axis (left to right), causing superimposition of hyperintensities on the bilateral adjacent brain parenchyma.

was the most common site (n = 58) (Fig 1), followed by the third ventricle (n = 47) (Fig 2) and the lateral ventricles (n = 13) (Fig 3). Twenty percent (n = 20) of subjects had VCSFA only in the fourth ventricle. When present in the third or fourth ventricles, VCSFA was usually prominent/severe (grade 2) (Figs 1 and 2). Lateral ventricular VCSFA was less common and less severe (usually grade 1). Lateral ventricular VCSFA was most commonly adjacent to the foramen of Monro (Fig 3). In one subject with severe VCSFA, both sagittal and axial FLAIR imaging was performed (Fig 1C and D); the severe VCSFA present in the fourth ventricle on axial FLAIR images (Fig 1C) disappeared on sagittal FLAIR images (Fig 1D). Ghost pulsation of the VCSFA in the fourth, third, or lateral ventricles was also seen in several of the patients (Figs 1E, 2C, and 3C). When present, this ghost pulsation artifact always manifested in the phase-encoding axis (left-to-right on these axial images), causing superimposition of ghost hyperintensity on normal brain parenchyma.

Factors Related to VCSFA

Third Ventricular VCSFA Related to Fourth Ventricular VCSFA.—Third ventricular and fourth ventricular VCSFA significantly coexisted: 75% of subjects who had VCSFA in the third ventricle also had VCSFA in the fourth ventricle ($P < .0001$). The severity of fourth ventricular VCSFA correlated positively and significantly with the severity of third ventricular VCSFA ($r = .38$, $P < .0001$). The group with fourth ventricular VCSFA had significantly more severe third ventricular VCSFA than did the group without fourth ventricular VCSFA ($P < .0001$). The group with third ventricular VCSFA had significantly more severe fourth ventricular VCSFA than did those without third ventricular VCSFA ($P < .0005$). Sex was not significantly associated with the severity or presence of VCSFA in any manner ($P > .10$)

Third Ventricular Size and Age Related to VCSFA.—Increasing third ventricular size and, to a lesser extent, increasing age were each significantly associated with VCSFA. The relationship between third ventricular size and VCSFA is shown in the Table and in Figure 4. The group with VCSFA in the ventricular system (n = 72) had significantly larger third ventricles ($P = .02$) but no difference in age ($P = .60$) as compared with those without VCSFA (n = 28). The group with third ventricular VCSFA had significantly larger third ventricles ($P < .0001$) and nonsignificantly greater age ($P = .08$) as compared with those without third ventricular VCSFA. The group with fourth ventricular VCSFA had significantly larger third ventricles ($P < .01$) and significantly greater age ($P < .05$) as compared with those without fourth ventricular VCSFA. Third ventricular size correlated significantly and positively with VCSFA severity in the third ventricle ($r = .45$, $P < .0001$), with VCSFA severity in the fourth ventricle ($r = 0.2$, $P = .03$), and with age ($r = .58$, $P < .0001$).

Discussion

The present study is a survey of the topography of VCSFA on axial FLAIR MR images. Our findings indicate that VCSFA is common on axial fast FLAIR images throughout the ventricular system in adult subjects of all ages. VCSFA is especially prominent and common in the fourth ventricle (Fig 1) and third ventricle (Fig 2) and is related to increasing third ventricular size and advancing age (Fig 4). VCSFA in the third and fourth ventricles

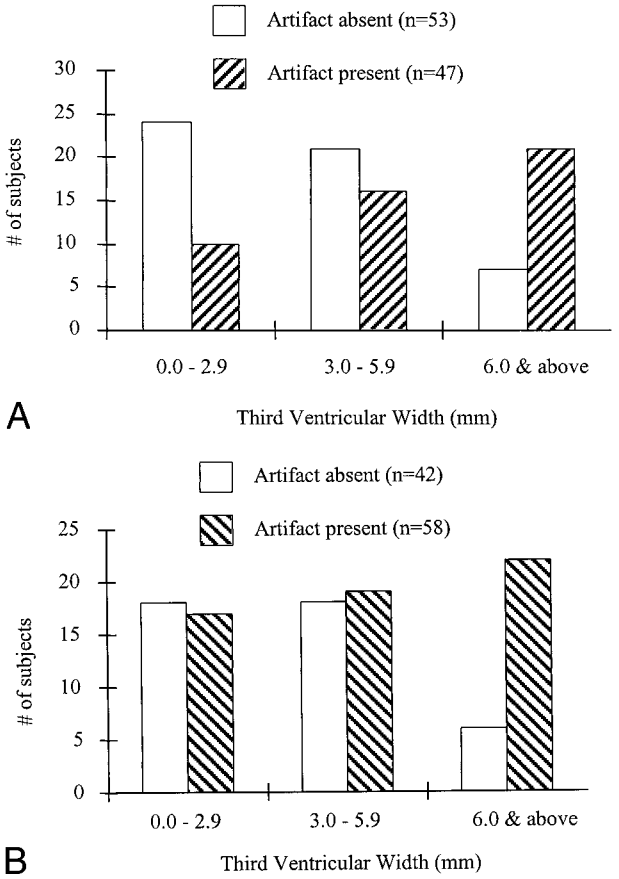

FIG 4. *A,* The group with third ventricular VCSFA had significantly larger third ventricles ($P < .0001$) than did those without third ventricular VCSFA. For illustrative purposes, the patients are divided into categories based on small, medium, and large third ventricles.

B, The group with fourth ventricular VCSFA had significantly larger third ventricles ($P < .01$) than did those without fourth ventricular VCSFA. For illustrative purposes, the patients are divided into categories based on small, medium, and large third ventricles.

is severe and could potentially reduce the sensitivity and specificity of axial FLAIR images in the evaluation of ventricular lesions. These findings suggest that altered CSF flow dynamics that occur with ventriculomegaly and aging contribute to VCSFA on axial FLAIR images.

We believe that the most important contributor to VCSFA is inflow of non-nulled CSF from the superior or inferior areas. This is analogous to the signal produced by the inflow of fresh blood on time-of-flight MR angiograms, only instead of saturation effects, the VCSFA is due to effects of inversion delay. CSF enters the brain sections between the inversion pulse and the beginning of signal sampling, is not properly nulled, and remains hyperintense on axial FLAIR images (2). The increased severity and frequency of VCSFA in the third and fourth ventricles is most likely multifactorial. One likely cause is the reflux of spinal CSF into these inferior ventricles through the posterior fossa. A second factor is increased velocity of CSF flow through the third and fourth ventricles, increasing the rate of superior entry of CSF from the lateral ventricles during inversion delay. Ghost pulsation effects also appear to contribute to VCSFA. Because CSF is moving in the ventricles, any residual non-nulled CSF will cause pulsation artifact in many places. One manifestation of this ghosting is the placement of redundant CSF signal across the phase-encoding axis in a manner that could obscure or mimic brain parenchymal lesions (Figs 1E, 2C, and 3C). Inflow and ghost pulsation effects are artifacts caused by flow, and are thus related. The difference is that optimal gradient moment nulling (eg, accounting for velocity, acceleration, jerk, and so on) might reduce the effect of ghosting but would not affect inversion delay artifact. Conversely, wider inversion pulses might help reduce the signal from inflowing CSF, but any moving protons will still cause ghosting of whatever signal they may contribute.

A limitation of this study is that we did not formally study the effect of altering our axial FLAIR parameters on VCSFA. We spent the year previous to the current study optimizing the axial FLAIR protocol at our center for scanning time, lesion contrast, and artifact. We found the current protocol to be optimal. Further adjustments in this protocol might reduce VCSFA on axial images. First, a wider slice-selective inversion section could be used and increased by 50% more than the imaging section to increase the inversion of CSF outside the imaging section while minimizing the cross-talk from one section to another. The use of other section-selective inversion pulses, non-section-selective inversion pulses, gradient moment nulling in the section-select direction, or the use of cardiac synchronization may also reduce CSF pulsation artifacts (1, 3) The increased scanning time caused by these adjustments might be offset by slightly lowering the TR, with acceptable loss of tissue contrast. These more conservative protocol adjustments may be especially useful in imaging elderly patients, those with ventriculomegaly, or those in whom lesions are suspected (eg, cases of hemorrhage). The quantification of VCSFA will also depend on chance synchronization of CSF flow during the period in which the sequence traverses the center of k-space. Therefore, the results from another set of 100 healthy subjects could be different on this machine or on a scanner produced by a different vendor. Further study of the use of other FLAIR parameters on a variety of scanners will be necessary to confirm and extend our findings. Subarachnoid space CSF artifact (Fig 1B and C) is also a pitfall of FLAIR imaging (1). It will be of interest to determine in future studies whether a relationship exists between subarachnoid space artifact and VCSFA or ventricular size.

In one of our patients, severe VCSFA was present on axial images but disappeared on sagittal sequences (Fig 1C and D). This is most likely because sagittal imaging will cause the necessary nulling of in-plane midline brain and cervical spi-

nal CSF before the fluid reaches the third and fourth ventricles during readout (ie, CSF flow remains in-plane and no inflow of non-nulled CSF occurs). We did not study ventricular pathologic conditions that might alter VCSFA or that could be masked by VCSFA, such as hemorrhage (8), infection/empyema, neoplasia, or normal-pressure hydrocephalus. Further study of the role of sagittal imaging in distinguishing VCSFA from pathologic ventricular disease is warranted.

We found that increased third ventricular size and age are related to increased severity and frequency of VCSFA. This ventriculomegaly and aging most likely increases CSF velocity and increases the rate and the volume of entry of non-nulled CSF into axial sections from superior and inferior spaces, including reflux from the cervical subarachnoid space (9–13). Increased CSF flow velocity will increase inversion delay and ghosting effects. This effect of aging and ventriculomegaly on increased CSF flow velocity has been shown by previous investigators of CSF flow dynamics by using the aqueductal flow void sign (12) or phase-contrast CSF flow quantification technique (13). One reason for this increased velocity is that as ventricular size increases with aging, the change in the cross-sectional area of the ventricles relative to the normal state is much greater than the change in the size of the cerebral aqueduct or the ventricular foramina relative to their normal state (9). Accordingly, the velocity of CSF flow in the foramina increases as the ventricular size increases (9). Studies have shown increased passage of subarachnoid dye into the fourth ventricle from the cisterna magna in patients with ventriculomegaly, owing to brain volume loss (ex-vacuo hydrocephalus) (11). This reflux may be enhanced in pathologic obstructive hydrocephalic states such as normal-pressure hydrocephalus (11) and pyogenic meningitis (14). Decreased compliance of periventricular tissues in the aging brain may allow for more vigorous transmission of systolic and diastolic pulsations to the ventricles, further increasing CSF velocity (9). Forceful CSF pulsations that occur in synchrony with systole and diastole appear to exert their maximal force at the base of the brain through the third ventricle (9), where CSF velocities are also maximal. Therefore, the contribution of aging and ventriculomegaly to the development of VCSFA is most likely multifactorial. VCSFA was also present in younger subjects with smaller ventricles. Thus, when interpreting axial FLAIR images of patients of all ages, the presence of hyperintensity in the ventricles could indicate artifact.

Conclusion

VCSFA on axial FLAIR images most likely represents inflow artifact due to inversion delay and ghosting effects. VCSFA is commonly found in the third and fourth ventricles, and less commonly in the lateral ventricles on axial FLAIR images. This artifact is often severe when present in the third and fourth ventricles and could obscure or mimic intraventricular disease. Although common in persons of all ages, VCSFA is related to advancing age and increasing ventricular size. Thus, altered CSF flow dynamics that occur with ventriculomegaly and aging contribute to VCSFA on FLAIR images and may necessitate compensatory adjustments in FLAIR protocol.

References

1. De Coene B, Hajnal JV, Gatehouse P, et al. **MR of the brain using fluid-attenuated inversion recovery (FLAIR) pulse sequences.** *AJNR Am J Neuroradiol* 1992;13:1555–1564
2. Ryberg JN, Hammond CA, Grimm RC, et al. **Initial clinical experience in MR imaging of the brain with a fast fluid-attenuated inversion recovery pulse sequence.** *Radiology* 1994;193: 173–180
3. Adams JG, Melhem ER. **Clinical usefulness of T2-weighted fluid-attenuated inversion recovery MR imaging of the CNS.** *AJR Am J Roentgenol* 1999;172:529–536
4. Alexander JA, Sheppard S, Davis PC, Salverda P. **Adult cerebrovascular disease: role of modified rapid fluid-attenuated inversion-recovery sequences.** *AJNR Am J Neuroradiol* 1996;17: 1507–1513
5. Filippi M, Horsfield MA, Rovaris M, et al. **Intraobserver and interobserver variability in schemes for estimating volume of brain lesions on MR images in multiple sclerosis.** *AJNR Am J Neuroradiol* 1998;19:239–244
6. Thurnher MM, Thurnher SA, Fleischmann D, et al. **Comparison of T2-weighted and fluid-attenuated inversion-recovery fast spin-echo MR sequences in intracerebral AIDS-associated disease.** *AJNR Am J Neuroradiol* 1997;18:1601–1609
7. Bakshi R, Bates VE, Mechtler LL, Kinkel PR, Kinkel WR. **Occipital lobe seizures as the major clinical manifestation of reversible posterior leukoencephalopathy syndrome: magnetic resonance imaging findings.** *Epilepsia* 1998;39:295–299
8. Bakshi R, Kamran S, Kinkel PR, et al. **Fluid-attenuated inversion-recovery MR findings in acute and subacute cerebral intraventricular hemorrhage.** *AJNR Am J Neuroradiol* 1999;20: 629–636
9. Sherman JL, Citrin CM, Gangarosa RE, Bowen BJ. **The MR appearance of CSF flow in patients with ventriculomegaly.** *AJR Am J Roentgenol* 1987;148:193–199
10. Bradley WG. **Magnetic resonance imaging in the evaluation of cerebrospinal fluid flow abnormalities.** *Magn Res Q* 1992;8: 169–196
11. Cummings JL, Benson DF. ***Dementia: A Clinical Approach.*** Stoneham: Butterworth-Heinemann; 1992:361–362
12. Bradley WG, Whittemore AR, Kortman KE, et al. **Marked cerebrospinal fluid void: indicator of successful shunt in patients with suspected normal-pressure hydrocephalus.** *Radiology* 1991;178:459–466
13. Bradley WG, Scalzo D, Queralt J, Nitz WN, Atkinson DJ, Wong P. **Normal-pressure hydrocephalus: evaluation with cerebrospinal fluid flow measurements at MR imaging.** *Radiology* 1996;198:523–529
14. Bakshi R, Kinkel PR, Mechtler LL, Bates VE. **Cerebral ventricular empyema associated with severe adult pyogenic meningitis: computed tomography findings.** *Clin Neurol Neurosurg* 1997;99:252–255